(d, 1 H, H-5), 6.15 (d, 1 H, H-1'), 6.45 (bs, 2 H, NH_2), 7.79 (s, 1 H, H-6). Anal. ($C_{26}H_{45}N_3O_8SSi_2$) C, H, N.

Antiretrovirus Assays. HIV-1 was originally obtained from the culture supernatant of the persistently HIV-infected H9 cell line (H9/HTLV-III_B),[65] which was kindly provided by R. C. Gallo and M. Popovic (National Institutes of Health, Bethesda, MD). Virus stocks were prepared from the supernatants of HIV-1-infected MT-4 cells.

MT-4 cells are human T-lymphocyte cells transformed by HTLV-1 and highly susceptible to the cytopathic effect of HIV. The methodology of the anti-HIV assays has been described previously.[17,22] Briefly, MT-4 cells (5×10^5 cells/mL) were suspended in fresh culture medium and infected with HIV-1 at 100 times the 50% cell culture infective dose ($CCID_{50}$) per milliliter of cell suspension. Then 100 μL of infected cell suspension was transferred to microtiter plate wells and mixed with 100 μL of the appropriate dilutions of test compounds. After 5 days, the number of viable cells for both virus-infected and mock-infected cell cultures was determined in a blood-cell-counting chamber by trypan blue staining. The 50% effective concentration (EC_{50}) and 50% cytotoxic concentration (CC_{50}) were defined as the compound concentrations required to reduce by 50% the number of viable cells in the virus-infected and mock-infected cell cultures, respectively.

(65) Popovic, M.; Sarngadharan, M. G.; Read, E.; Gallo, R. G. Detection, Isolation, and Continuous Production of Cytopatic Retroviruses (HTLV-III) from Patients with AIDS and Pre-AIDS. *Science* **1984**, *224*, 497–500.

Acknowledgment. We thank María Jesús Moreno, Ann Absillis, and Lizette van Berckelaer for their excellent technical assistance. We thank Mr. Francisco Caballero for processing the manuscript. We also thank the Residencia de Estudiantes and Ayuntamiento de Madrid for a grant to M.J.P. This research was supported in part by the Programa Nacional de Investigación y Desarrollo Farmacéutico of Spain (Project FAR88-01606/1), the AIDS Basic Research Programme of the European Community, and by grants from the Belgian Fonds voor Geneeskundig Wetenschappelijk Onderzoek (Projects 3.0097.87 and 3.0026.91), and the Belgian Geconcerteerde Onderzoeksacties (Project 90/94-2).

Registry No. 1, 6698-46-0; 3, 142131-02-0; α-4, 142102-69-0; β-4, 142102-70-3; 5a, 142102-71-4; 5b, 142102-72-5; 5c, 142102-73-6; 6a, 142102-74-7; 7a, 141781-18-2; 8a, 141781-17-1; 8b, 141845-83-2; 8c, 142102-75-8; 9a, 141684-47-1; 10a, 142102-76-9; 11, 142102-77-0; 12, 142102-78-1; 13, 142102-79-2; 14, 142102-80-5; 15, 142102-81-6; 16, 142102-82-7; 17, 142102-83-8; thymine, 65-71-4; uracil, 66-22-8.

Template-Directed Design of a DNA–DNA Cross-Linker Based upon a Bis-Tomaymycin–Duplex Adduct

Jeh-Jeng Wang, G. Craig Hill, and Laurence H. Hurley*

College of Pharmacy, The Drug Dynamics Institute, University of Texas at Austin, Austin, Texas 78712.
Received March 13, 1992

A template-directed approach to the design of a DNA–DNA interstrand cross-linker based upon the structure of a bis-tomaymycin–duplex adduct has been carried out. Tomaymycin is a member of the pyrrolo[1,4]benzodiazepines antitumor antibiotics. In a previous study (F. L. Boyd et al., *Biochemistry* 1990, *29*, 2387–2403), we have shown that two tomaymycin molecules can be covalently bound to a 12-mer duplex molecule, where the drug molecules are on opposite strands six base-pairs apart, and the stereochemistry at the drug bonding site, and orientation in the minor groove, was defined by high-field NMR. This bis-tomaymycin 12-mer duplex adduct maintains the self-complementarity of the duplex and a B-type structure. In the present study we have shown using high-field NMR that this same 12-mer sequence can be truncated by two base pairs so that the two tomaymycin-modified guanines are now only four base-pairs apart, the two species of tomaymycin molecules are still bound with the same stereochemistry and orientation, and the 10-mer duplex adduct maintains its self-complementarity. In a second 10-mer duplex we have shown that changing the bonding sequence from 5'CGA to 5'AGC does not significantly affect the structure of the bis-tomaymycin–duplex adduct. However, when the sequence is rearranged so that the drugs point in a tail-to-tail orientation rather than in the previous head-to-head configuration, there are more than one species of tomaymycin bound to DNA, and, as a consequence, the bis-tomaymycin 10-mer duplex adduct loses its self-complementarity. Last, we have used the 10-mer duplex containing the 5'CGA sequence, in which the tomaymycin molecules are oriented head to head, to design an interstrand cross-linking species in which the two drug molecules are linked together with a flexible linker molecule.

Introduction

Anthramycin, tomaymycin (I), and sibiromycin are the best known examples of the naturally occurring pyrrolo[1,4]benzodiazepines (P[1,4]B).[1-3] These antibiotics react covalently with DNA to form an N2-guanine adduct that lies within the minor groove of DNA (Figure 1).[4,5] The P[1,4]Bs are not only specific for N2 of guanine, but are only reactive with guanines in certain sequences, and therefore show sequence selectivity.[6,7] The most favored sequences for bonding are 5'PuGPu with 5'PyGPu and 5'PuGPy of intermediate reactivity (Pu = purine; Py = pyrimidine), while 5'PyGPy sequences show the least reactivity. In principle, there are four species of covalently bound adducts that can occur as the two 11*S* enantiomers, in which the aromatic ring of the drug lies either to the

* Address correspondence to this author or call (512)471-4841.

(1) Remers, W. A. In *The Chemistry of Antitumor Antibiotics*; Wiley: New York, 1988; Vol. 2, pp 28–92.
(2) Thurston, D. E.; Hurley, L. H. A Rational Basis for Development of Antitumor Agents in the Pyrrolo(1,4)benzodiazepine Group. *Drugs Future* 1984, *8*, 957–971.
(3) Remers, W. A.; Barkley, M. D.; Hurley, L. H. Pyrrolo(1,4)-benzodiazepines. Unraveling the Complexity of the Structures of the Tomaymycin-DNA Adducts in Various Sequences Using Fluorescence, ^{1}H-NMR, and Molecular Modeling. A chapter in *Nucleic Acid Targeted Drug Design*; Perun, T., Propst, C., Eds.; Marcel Dekker, Inc.: New York, 1992, in press.
(4) Hurley, L. H.; Petrusek, R. Proposed Structure of the Anthramycin-DNA Adduct. *Nature (London)* 1979, *282*, 529.

0022-2623/92/1835-2995$03.00/0

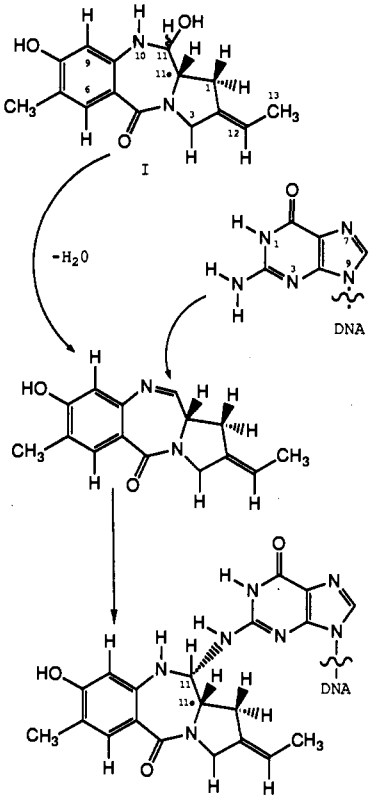

Figure 1. Proposed reaction of tomaymycin (I) with DNA to form the (N2) guanine DNA adduct.[11]

3′ or 5′ direction, and as the two equivalent 11*R* enantiomers. For anthramycin we have shown that in all the bonding sequences so far examined, which are representative of all four groups, the species of drug found on DNA is the 11*S*,3′ species.[8,9] For tomaymycin the situation is more complex, because on the least favored sequence, 5′PyGPy, tomaymycin exists as a 50:50 mixture of the 11*S* and 11*R* enantiomers, while on 5′CGA only the 11*S*3′ species is found.[10,11]

Scheme I

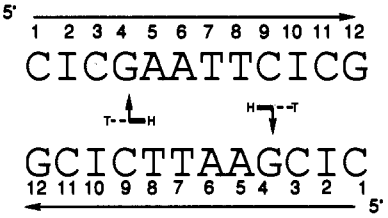

As would be expected for DNA-reactive compounds, the P[1,4]Bs show potent antitumor activity.[12] In a comparison study, tomaymycin showed the most potent cytotoxicity in inhibition of proliferation of B16 melanoma cells, but anthramycin showed the highest increase in life span of mice bearing P388 leukemia cells.[7] Other simpler synthetic analogs generally show reduced in vitro and in vivo potency.[7] Although anthramycin has the best antitumor activity, it produces cardiotoxicity, which has precluded its continued clinical application.[13] The relatively poor antitumor profile of the synthetic analogs of the P[1,4]B encouraged us to examine the possibility of designing DNA–DNA cross-linkers that would be expected to be more biologically potent and have increased sequence specificity. As a first step to the design of a P[1,4]B interstrand cross-linker, we have characterized a bis-tomaymycin 12-mer duplex adduct (Scheme I), in which the drugs are covalently bound six base pairs apart on opposite strands.[11] The results of this study were encouraging. The 12-mer duplex maintained its self-complementarity following drug bonding, and the duplex showed relatively little distortion, which should facilitate computer-aided drug design. In the present study, we have examined three further questions relating to the design of DNA–DNA interstrand cross-linkers based upon tomaymycin. First, what is the shortest distance between the drug molecules that can be achieved without preventing bis-adduct formation and loss of self-complementarity? Second, what effect does changing the bonding sequence from 5′CGA to 5′AGC have on the species of tomaymycin bound? Third, can tomaymycin molecules be bound in a tail-to-tail orientation rather than head-to-head, as previously defined? On the basis of these results, we have designed a DNA–DNA interstrand cross-linker using computer-aided drug design that should react specifically at guanines four base pairs apart on opposite strands without serious distortion of the duplex. A DNA–DNA interstrand cross-linker (DSB-120) has been synthesized and shown to cross-link as predicted and be much more potent than any of the monoalkylation compounds (see later).

Experimental Section

Chemicals. (11*R*,11a*S*)-Tomaymycin 11-methyl ether (TME) was a generous gift from Dr. Kohsaka of Fujisawa Pharmaceuticals. The DNA oligomers were synthesized in-house on an automated DNA synthesizer (Applied Biosystems 381A) using a solid-phase cyanoethyl phosphoramidite approach. Reagents used to prepare NMR buffer and solvents, sodium phosphate

(5) Petrusek, R. L.; Anderson, G. L.; Garner, T. F.; Fannin, Q. L.; Kaplan, D. J.; Zimmer, S. G.; Hurley, L. H. Pyrrolo(1,4)-benzodiazepine Antibiotics. Proposed Structures and Characteristics of the *In Vitro* DNA Adducts of Anthramycin, Tomaymycin, Sibiromycin, and Neothramycins A and B. *Biochemistry* **1981**, *20*, 1111–1119.
(6) Hertzberg, R.; Hecht, S.; Reynolds, V. L.; Molineux, I. J.; Hurley, L. H. DNA Sequence Specificity of the Pyrrolo(1,4)-benzodiazepine Antitumor Antibiotics. MPE Fe(II) Footprinting Analysis of DNA Binding Sites for Anthramycin and Related Drugs. *Biochemistry* **1986**, *25*, 1249–1258.
(7) Hurley, L. H.; Reck, T.; Thurston, D. E.; Holden, K. G.; Hertzberg, R. P.; Hoover, J. R. E.; Gallagher, G., Jr.; Faucette, L. F.; Mong, S-M.; Johnson, R. K. Pyrrolo(1,4)benzodiazepines Antitumor Antibiotics. Relationship of DNA Binding and Sequence Specificity to Biological Activities of Natural and Synthetic Compound. *Chem. Res. Toxicology* **1988**, *1*, 258–268.
(8) Boyd, F. L.; Cheatham, S. F.; Remers, W.; Hill, G. C.; Hurley, L. H. Characterization of Structure of the Anthramycin-d-(ATGCAT)$_2$ Adduct by NMR and Molecular Modeling Studies. Determination of the Stereochemistry at the Covalent Linkage Site, Orientation in the Minor Groove, and Effect of Drug Binding on Local DNA Structure. *J. Am. Chem. Soc.* **1990**, *112*, 3279–3289.
(9) Mountzouris and Hurley, unpublished results.
(10) Cheatham, S. F.; Kook, A. M.; Hurley, L. H.; Barkley, M.; Remers, W. One- and Two-Dimensional ^{1}H-NMR Fluorescence and Molecular Modeling Studies on the Tomaymycin-d(ATGCAT)$_2$ Adduct. Evidence for Two Covalent Adducts with Opposite Orientations and Stereochemistry at the Covalent Linkage Site. *J. Med. Chem.* **1988**, *31*, 583–590.
(11) Boyd, F. L.; Stewart, D.; Remers, W. A.; Barkley, M. D.; Hurley, L. H. Characterization of a Unique Tomaymycin-d-(CICGAATTCICG)$_2$ Adduct Containing Two Drug Molecules per Duplex by NMR, Fluorescence, and Molecular Modeling Studies. *Biochemistry* **1990**, *29*, 2387–2403.
(12) Hurley, L. H. Pyrrolo(1,4)benzodiazepine Antitumor Antibiotics. Comparative Aspects of Anthramycin, Tomaymycin, and Sibiromycin. *J. Antibiot.* **1977**, *30*, 349–370.
(13) Cargill, C.; Bachmann, E.; Zbinden, G. Effects of Daunomycin and Anthramycin on Electrocardiogram and Mitochondrial Metabolism of the Rat Heart. *J. Natl. Cancer Inst.* **1974**, *53*, 481–486.

Table I. Energies (kcal/mol) of Covalent Complexes between Tomaymycin and d(CICGATCICG)$_2$

direction of aryl ring	config at C-11	drug–drug orientation	total energy	intermolecular			distortion			net bonding energy[e]
				vdw[a]	elstat[b]	total	helix[c]	drug[d]	total	
3′	R	head–head	−675.6	−32.4	−22.2	−54.6	+17.8	+14.6	+32.4	−22.2
3′	S	head–head	−703.6	−42.9	−29.9	−72.8	+16.3	+7.4	+23.7	−49.1
5′	R	tail–tail	−688.5	−36.4	−45.2	−81.6	+32.7	+15.0	+47.7	−33.9
5′	S	tail–tail	−703.6	−45.8	−32.3	−78.1	+10.5	+18.5	+29.0	−49.1

[a] Van der Waals or steric contribution. [b] Electrostatic contribution. [c] The enthalpy of d(CICGATCICG)$_2$ is −698.3 kcal/mol. [d] The enthalpy of the drug molecule in the absence of the DNA is +22.4 kcal/mol. [e] Net bonding is the total intermolecular bonding plus helix and drug distortion.

(99.99%), sodium chloride (99.99%), and D_2O (99.99%) were purchased from Aldrich Co. High-performance liquid chromatography (HPLC) grade water and methanol were purchased from Baxter Scientific and Fisher Co., respectively. Hydroxyapatite used to purify the duplex and duplex-adducts was purchased from Cal Biochem Co. Sephadex G-25 (superfine) was purchased from Pharmacia Co. Sep-Pak cartridges (C18) were purchased from Waters Co.

Preparation of Duplex Decanucleotides. Single strands were synthesized in-house on an Applied Biosystems automated DNA synthesizer Model 381A. Sample deprotection with saturated ammonium hydroxide solution (55 °C overnight) was followed by evaporation at room temperature. The single strands were annealed in a sealed vial, containing 1 mL of NMR buffer (10 mM NaH_2PO_4, and 100 mM NaCl) by heating to 70 °C followed by cooling to room temperature overnight. The crude oligomers were purified on hydroxyapatite (25 × 3 cm) with a gradient of 10–200 mM sodium phosphate buffer (pH 6.85) at room temperature to remove any excess single-stranded oligomers. The 10-mer duplexes (25–35 mg) were then lyophilized and redissolved in 3–5 mL of HPLC grade water and desalted on a column of Sephadex G-25 (superfine) by elution with HPLC water. The desalted oligomers were then lyophilized to dryness and redissolved in 0.5 mL of NMR buffer. The samples were lyophilized to dryness and redissolved in 0.5 mL of 99.99% D_2O and transferred into a 5-mm ultrathin NMR tube.

Preparation of Tomaymycin 10-Mer Duplex Adducts. TME (~6 mg) dissolved in 0.2 mL of DMF was added to 25–35 mg of purified 10-mer duplex in 0.5 mL of 20 mM sodium phosphate and 200 mM sodium chloride buffer (pH 6.85). The reaction mixtures were stirred at room temperature for 5 days in the dark, lyophilized to dryness, redissolved in 1.0 mL of HPLC grade water, and applied to hydroxyapatite columns (25 × 3 cm). Elution with a gradient of 10–200 mM sodium phosphate buffer (pH 6.85) at room temperature removed free drug and other impurities. The solutions containing the pure adducts were lyophilized, redissolved in 0.5 mL of NMR buffer, lyophilized, and redissolved in 0.5 mL of 99.99% D_2O and transferred into 5-mm ultrathin NMR tubes.

NMR Spectroscopy. One- and two-dimensional ^1H and ^{31}P NMR data sets were recorded on a General Electric GN-500 FT NMR at room temperature. Chemical shifts were reported in parts per million and referenced relative to external trisodium phosphate (TSP) (1 mg/mL) in D_2O for ^1H and an external reference of 85% H_3PO_4 in D_2O for ^{31}P resonances. Mononuclear scalar coupling was determined by using the standard magnitude-correlated spectroscopy (COSY). 2K complex points in t_2 and 256 points in the t_1 domain were acquired with a repetition time of 0.5 s. Phase-sensitive two-dimensional nuclear Overhauser effect spectroscopy (NOESY) experiments were acquired similarly with a repetition time of 2.0 s. Mixing times of 125 and 250 ms were used for the phase-sensitive NOESY experiments and were stochastically varied to suppress cross-peaks arising from scalar coupling.[14] The data were zero filled in t_1 such that the final frequency domain spectra consisted of 1K × 1K data matrices after symmetrization. Proton-decoupled phosphorous spectra were collected at 202.44 MHz. Phosphorus-detected ^1H–^{31}P two-dimensional heteronuclear phase-sensitive correlation experiments were performed according to the procedure by Bax and Sarker.[15]

Molecular Modeling. The crystal structure of TME[16] provided the initial coordinates for these studies. Previous ab initio calculations with the methoxyl group removed yielded the partial atomic charges.[10] The drug structure was minimized using AMBER 3.0 revision A[17] and the all-atom force-field parameters[18] until the energy root mean square gradient was less than 0.1 kcal/mol Å with the nonbonded pairs cutoff of 99 Å and updated every 100 cycles. The DNA duplexes were constructed in AMBER from Arnott's B-DNA coordinates[19] and minimized under the same conditions described above. The minimized oligomers were then docked with two tomaymycin drug molecules via the program MidasPlus,[20] and the docked coordinates were used as input for minimization and then subjected to 55 ps of molecular dynamics at 300 ± 5 K in AMBER with a gradual increase in temperature from 10 to 300 K over the first five ps. Attempts at longer simulation times were made for two of the sixteen models. After 100 ps, the models were very similar to that found for the 50 ps trial, and upon minimization only slight differences existed between them. This would indicate that the system seems to converge to a common final complex. The resultant models were reminimized to <0.1 kcal/mol Å.

Results and Discussion

I. Shortening the Distance between the Tomaymycin Covalently Modified Guanines from Six to Four Base Pairs Is Allowed and the Self-Complementarity of the 10-Mer d(CICGATCICG)$_2$ Is Maintained. In a previous study using the 12-mer d(CIC*GAATTCICG)$_2$, we had shown that tomaymycin can bond to the two equivalent guanines indicated by an (*) on the opposite strands without losing the self-complementarity of the unmodified duplex.[11] In addition, we had shown that the species of tomaymycin–(N2-guanine)-DNA formed on the 12-mer has an 11*S* stereochemistry at the covalent modification site and is orientated with the aromatic ring of the drug to the 3′ side of the alkylated guanine (Scheme I). This 12-mer was designed based upon the well-characterized structure of the Dickerson dodecamer[21] [d(CGCGAATTCGCG)$_2$] in which the two guanines underlined were replaced with inosines. This sub-

(14) States, D. J.; Haberkorm, R. A.; Ruben, D. J. A Two-Dimensional Nuclear Overhauser Experiment with Pure Absorption. *J. Magn. Reson.* 1982, *48*, 286.

(15) Bax, A.; Sarker, S. K. Elimination of Refocusing Pulses in NMR Experiments. *J. Magn. Reson.* 1984, *60*, 170–176.

(16) Arora, S. K. Structure of Tomaymycin, a DNA-Binding Antitumor Antibiotic. *J. Antibiot.* 1981, *34*, 462–464.

(17) Seibel, G. L.; Singh, U. C.; Weiner, P. K.; Caldwell, J. W.; Kollman, P. A. AMBER 3.0 Revision A; Department of Pharmaceutical Chemistry, University of California, San Francisco, CA 94143 (1989).

(18) Weiner, S. J.; Kollmann, P. A.; Case, D.; Singh, U. C.; Ghio, C.; Alagona, G.; Prafeta, S., Jr.; Weiner, P. K. A New Force Field for Molecular Mechanical Simulation of Nucleic Acids and Proteins. *J. Am. Chem. Soc.* 1984, *106*, 765–784.

(19) Arnott, S.; Campbell-Smith, P.; Chandrasekaran, R. In *CRC Handbook of Biochemistry*; Fasmay, G. D., Ed.; CRC Press: Cleveland, 1976; Vol. 2, pp 411–422.

(20) Ferrin, T. E.; Avang, C. C.; Jarvis, L. E.; Langridge, R. The MIDAS Display System. *J. Mol. Graphics* 1988, *6*, 13–27.

(21) Drew, H. R.; Wing, R. M.; Takano, T.; Broka, C.; Tanaka, S.; Itakura, K.; Dickerson, R. E. Structure of a B-DNA dodecamer: Conformation and Dynamics. *Proc. Natl. Sci. U.S.A.* 1981, *78*, 2179–2183.

Scheme II

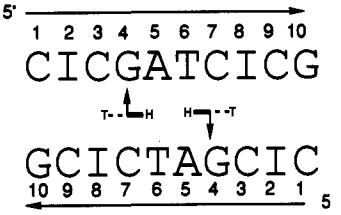

stitution was made because inosine differs from guanine in that it lacks the exocyclic 2-amino group and, consequently, is unreactive towards alkylation by tomaymycin. Since the structural analysis of this bis-tomaymycin 12-mer duplex adduct showed little distortion relative to the duplex alone (in fact, drug modification appeared to shift the overall structure of the duplex to a *more* idealized B form), it seemed likely that truncating the duplex between the two guanines by two A–T pairs might be possible, while still maintaining the overall structure of the duplex adduct, provided steric interactions between the two drug molecules did not occur. Consequently, the 10-mer (see Scheme II) was synthesized as a template for evaluation of this proposal. Partial characterization of duplex by high-field ^{1}H NMR revealed it to have an overall B-type structure (J.-J. Wang, unpublished results). This 10-mer to be modified by tomaymycin was first subjected to molecular modeling studies and subsequently analyzed by high-field ^{1}H and ^{31}P NMR.

A. Molecular Modeling of the Bis-tomaymycin 10-Mer[d(CICGATCICG)$_2$] Adduct. The four possible species (11*S*,3′; 11*S*5′; 11*R*,3′; and 11*R*,5′) of tomaymycin on the 10-mer were modeled using AMBER 3A. The results (Table I) show that of the four species modeled, the 11*S*,3′ is identical in net bonding energy to the 11*S*,5′ species. While the 11*S*,5′ species produces better intermolecular interactions than the 11*S*,3′ species, it also induces more distortion. Previous work using only molecular mechanics rather than molecular mechanics and molecular dynamics correctly predicted the species found experimentally.[8,10,11] The current study using molecular dynamics and molecular mechanics is more rigorous, introduces less bias into the experiments, and is therefore expected to provide improved data for predicting which bis-tomaymycin–duplex adduct is the most favored and why. Nevertheless, the use of counterions and solvent should provide even further improvements. Some attempts were made in this direction, but we encountered considerable problems with migration of chlorine from the DNA, which led to unrecoverable, poor trajectories.

B. ^{1}H and ^{31}P NMR Analysis of the Bis-tomaymycin 10-Mer Duplex (5′CGA) Adduct. (1) Self-Complementarity of the 10-Mer Duplex Adduct. A comparison of the one-dimensional ^{31}P NMR of the duplex and its bis-tomaymycin–duplex adduct is shown in Figure 2, parts A and B, respectively. While there is considerable overlap of resonance signals in the duplex, in the bis-adduct the ^{31}P NMR signals are well resolved and clearly show just nine discrete signals, indicating the duplex adduct maintains its self-complementarity following tomaymycin modification. The resonance signal for the phosphorous atom between ^{3}C and ^{4}G is shifted upfield, which was also previously found in the corresponding 12-mer duplex adduct.[11] The one-dimensional ^{1}H NMR also provided evidence for the maintenance of the self-complementarity of the bis-tomaymycin–duplex adduct (J.-J. Wang, unpublished results).

(2) Stereochemistry at the C-11 Covalent Linkage Site between Tomaymycin and the 10-Mer Duplex.

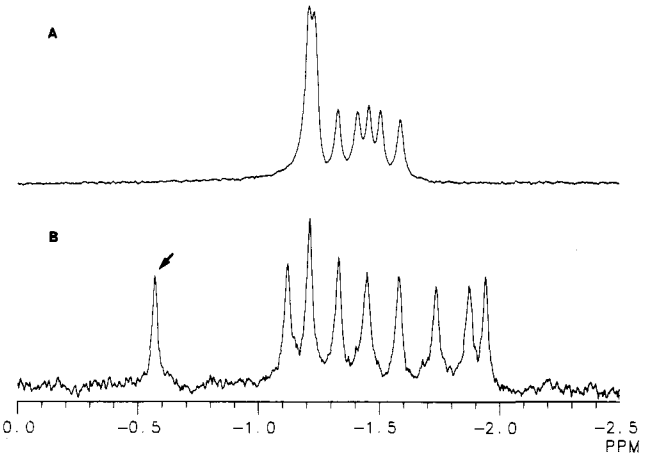

Figure 2. Proton-decoupled 202.44-MHz phosphorus NMR spectra (−2.5–0 ppm) of (A) the 10-mer duplex shown in Scheme II and (B) its bis-tomaymycin 10-mer duplex adduct in 0.5 mL of D_2O buffer containing 10 mM sodium phosphate and 100 mM sodium chloride, pH 6.85 at 23 °C. Arrowhead denotes upfield-shifted ^{3}C–^{4}G phosphorus resonance.

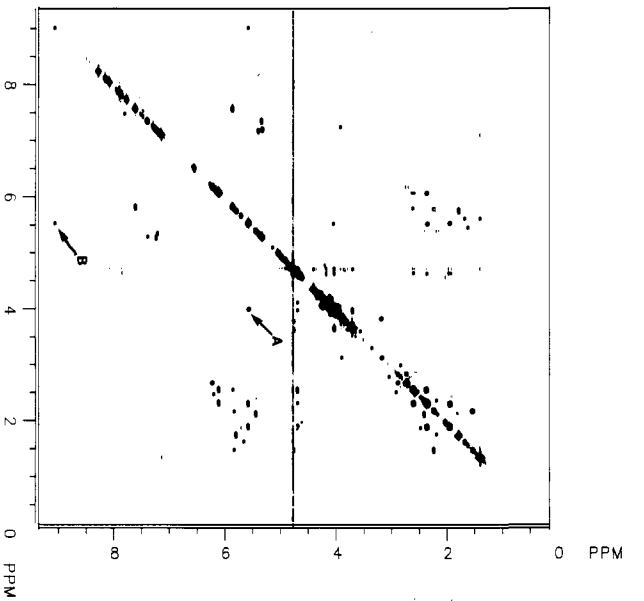

Figure 3. Two-dimensional magnitude COSY contour plot of the bis-tomaymycin 10-mer duplex adduct shown in Scheme II in 0.5 mL of D_2O buffer containing 10 mM sodium phosphate and 100 mM sodium chloride, pH 6.85 at 23 °C. Arrowhead A denotes the scalar coupling indicative of the 11*S* diastereomer between tomaymycin H11 and H11a protons. Arrowhead B denotes scalar coupling between the ^{4}G hydrogen-bonded amino proton and tomaymycin H11.

On the basis of molecular modeling, we have previously argued that *only* the 11*S*,11a*S* diastereomer of the tomaymycin–duplex adduct with the 3′ orientation will show scalar coupling between the C11 and C11a protons of tomaymycin.[11] This is because the 11*R*,11a*S* diastereomer has a dihedral angle between these protons of almost 90°. Examination of the magnitude COSY spectrum (Figure 3) of the bis-tomaymycin–d(CICGATCICG)$_2$ adduct shows scalar coupling of the 11 and 11a protons (cross-peak A), confirming the 11*S*,11a*S* diastereomer as the species found on the 10-mer, as was previously found for the 12-mer.[11] Cross-peak B in Figure 3 is due to the scalar coupling between the tomaymycin H11 proton and the exocyclic proton on N2 of guanine, which confirms the covalent linkage sites. The equivalent cross-peak was also evident in the 12-mer duplex adduct.[11] Examination of the nuclear

Table II. Selected Intermolecular NOE Contacts between Tomaymycin and d(CICGATCICG)$_2$

DNA proton	chemical shift[a]	tomaymycin proton	chemical shift[a]	NOE intensity[b]	distance in S, 3′ model[c]
^{5}AH2	8.05	H9	6.51	s	2.26
^{8}IH2	7.26	H13	1.74	m	3.24–5.01[d]
^{5}AH1′	6.15	H11	5.56	s	2.58
^{5}AH4′	4.23	H11	5.56	m	2.99

[a] Chemical Shifts are in ppm relative to external TSP in D_2O. [b] s = strong and m = medium (relative to cytosine H5 to H6 crosspeak intensities). [c] Distances are in angstroms. [d] Distances for methyl protons reported as a range (minimum–maximum) due to rotation.

Scheme III

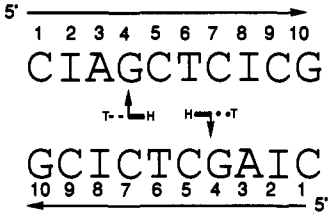

Overhauser effect (NOE) cross-peaks for H11 confirms the assignment of the *S* configuration (Table II). If tomaymycin adopts an 11*R* configuration upon bonding, then intermolecular NOEs would be expected between H11 and the H1′ and H4′ sugar protons of ^{8}I. Conversely, if tomaymycin adopts an 11*S* configuration upon bonding, the intermolecular NOEs would be expected between H11 and the H1′ and H4′ sugar protons of ^{5}A. The NMR data summarized in Table II shows a strong NOE between ^{5}AH1′ and H11 of tomaymycin and a medium NOE between ^{5}AH4′ and H11. NOEs were not observed between H11 and the equivalent ^{8}I sugar protons (J.-J. Wang, unpublished results); therefore, tomaymycin adopts an *S* configuration upon covalent bonding to the 5′CGA 10-mer as shown in Scheme II. A parallel set of intermolecular NOEs was used to assign the anthramycin stereochemistry on a 6-mer duplex adduct.[22]

(3) Orientation of the Tomaymycin Molecule on d(CICGATCICG)$_2$. The adenine and inosine H2 protons are located in the minor groove of DNA and are therefore reporter protons that can be used through NOE data to locate the orientation of the drug molecule on DNA. The ^{5}A and ^{8}I adenine H2s are located on the 3′ and 5′ sides, respectively, of the covalently modified guanine, and their NOEs into specific tomaymycin protons are indicative of the orientation of the drug in the minor groove. The NOEs listed in Table II show that while ^{5}AH2 shows an NOE into H9 of tomaymycin, ^{8}IH2 shows an NOE into H13 of tomaymycin. Therefore, the tomaymycin molecule is oriented with the aromatic ring of the drug molecule to the 3′ side of the covalently modified guanine. The upfield-shifted resonance signals of the 4′ proton of ^{5}A and the H5′ and H5″ protons of ^{8}I (J.-J. Wang, unpublished results) are due to their shielding by the aromatic ring of tomaymycin and thus confirms this orientation. In summary, the bis-tomaymycin 10-mer duplex adduct shown in Scheme II maintains the self-complementarity, stereochemistry, and orientation specificity shown previously in the 12-mer duplex adduct,[11] and this is one of the two species (11*S*,3′ and 11*S*,5′) predicted by molecular modeling.

II. What Effect Does Changing the Tomaymycin Bonding Sequence from 5′CGA to 5′AGC Have on the

(22) Krugh, T. R.; Graves, D. E.; Stone, M. P. Two-Dimensional NMR Studies on the Anthramycin-d(ATGCAT)$_2$ Adduct. *Biochemistry* **1989**, *28*, 9988–9994.

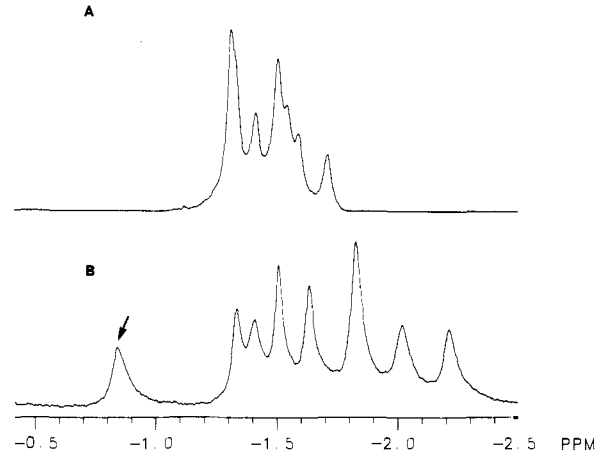

Figure 4. Proton-decoupled 202.44-MHz phosphorus NMR spectra (−2.5–0.5 ppm) of (A) the 10-mer duplex shown in Scheme III and (B) its bis-tomaymycin 10-mer duplex adduct in 0.5 mL of D_2O buffer containing 10 mM sodium phosphate and 100 mM sodium chloride, pH 6.85 at 23 °C. Arrowhead denotes upfield-shifted ^{5}C–^{6}I phosphorus resonance.

Species of Tomaymycin Attached to the 10-Mer? To gain a limited appreciation for how the bonding sequence effects the orientation and stereochemistry of the covalently bound species of tomaymycin, a second bonding sequence, 5′AGC (see Scheme III), was evaluated for the species of tomaymycin–DNA adduct formed and maintenance of duplex self-complementarity. This sequence belongs to the PuGPy group, which, along with 5′CGA (PyGPu), is the intermediately favored bonding sequence for tomaymycin.[6]

A. Molecular Modeling of the Bis-tomaymycin 10-Mer[d(CIAGCTCICG)$_2$] Adduct. The four possible combinations (11*S* and 11*R*, 3′ and 5′) of tomaymycin on the 10-mer in Scheme III were modeled using AMBER 3A. The results (Table III) show that the 11*S*,5′ species is predicted to be the product. This species is predicted to be 14.2 kcal/mol Å more stable than the next best species (11*S*,3′) mainly due to increased steric interactions.

B. ^{1}H and ^{31}P NMR Analysis of the Bis-tomaymycin 10-Mer Duplex (5′AGC) Adduct. (1) In the duplex alone, the signals are dispersed between −1.3 to −1.8 ppm, while in the duplex adduct they are more widely dispersed between −0.9 to −2.3 ppm (Figure 4, parts A and B). In the bis-tomaymycin–duplex adduct there are eight well-resolved ^{31}P resonance signals with two signals being superimposed at −1.85 ppm, giving a total of nine phosphate resonances, which demonstrates the self-complementarity of the duplex adduct. As was found for the 10-mer duplex adduct having the 5′CGA bonding, one of the ^{31}P resonance signals is moved downfield, but in this case it is the phosphate between two bases to the 3′ side of the covalently modified guanine (i.e., ^{5}C–^{6}I). This is different from the 5′CGA sequence, where it was found to be the ^{3}C–^{4}G phosphorus resonance signal. The self-complementarity is also evident from magnitude COSY that shows four scalar cross-peaks for the 4 cytosine 5H–6H protons (box A in Figure 5).

(2) Stereochemistry at C-11 and Orientation of Tomaymycin in the Minor Groove of DNA. Similar arguments to that made previously for the bis-tomaymycin 12-mer duplex adduct[11] and the 10-mer in Scheme II can be used to assign the stereochemistry at C11 as *S* for tomaymycin in the 5′AGC sequence; i.e., the scalar cross-peak (arrow in Figure 5) identified for the C11 and C11a protons occurs at 3.78 and 5.56 ppm. The 11*S* stereochemistry is also confirmed by the NOE cross-peak in-

Table III. Energies (kcal/mol) of Covalent Complexes between Tomaymycin and d(CIAGCICTCG)$_2$

direction of aryl ring	config at C-11	drug–drug orientation	total energy	intermolecular			distortion			net bonding energy[e]
				vdw[a]	elstat[b]	total	helix[c]	drug[d]	total	
3′	R	head–head	−690.4	−38.0	−31.8	−69.8	+1.5	+19.0	+20.5	−49.3
3′	S	head–head	−699.9	−42.0	−27.6	−69.6	+3.6	+8.3	+11.9	−57.7
5′	R	tail–tail	−697.4	−41.9	−34.0	−75.9	+4.3	+15.2	+19.5	−56.4
5′	S	tail–tail	−714.1	−51.7	−28.8	−80.5	+1.4	+7.2	+8.6	−71.9

[a] Van der Waals or steric contribution. [b] Electrostatic contribution. [c] The enthalpy of d(CIAGCICTCG)$_2$ is −681.4 kcal/mol. [d] The enthalpy of the drug molecule in the absence of the DNA is +22.4 kcal/mol. [e] Net bonding is the total intermolecular bonding plus helix and drug distortion.

Table IV. Selected Intermolecular NOE Contacts between Tomaymycin and d(CIAGCTCICG)$_2$

DNA proton	chem. shift[a]	tomaymycin proton	chem. shift[a]	NOE inten[b]	distance in S, 3′ model[c]
^{6}IH2	7.84	H9	6.30	s	2.68
^{3}AH2	7.44	H13	1.75	m	2.10–3.86[d]
^{5}CH1′	5.32	H11	5.56	s	2.65
^{5}CH4′	5.73	H11	5.56	m	3.17

[a] Chemical shifts are in ppm relative to external TSP in D_2O. [b] s = strong and m = medium (relative to cytosine H5 to H6 cross-peak intensities). [c] Distances are in angstroms. [d] Distances for methyl protons reported as a range (minimum–maximum) due to rotation.

tensities between ^{5}CH1′ and ^{5}CH4′ and the H11 protons of tomaymycin (Table IV). ^{3}AH2 and ^{6}IH2 provide the reporter atoms in the minor groove to the 5′ and 3′ sides of the covalently modified guanine (^{4}G) and show NOEs to the H13 and H9 protons of tomaymycin, respectively (Table IV). This confirms that the orientation of tomaymycin in this duplex is with the aromatic ring to the 3′ side of the covalently modified guanine. In summary for bonding sequences of intermediate selectivity (i.e., 5′PyGPu and 5′PuGPy) in the examples tested (5′CGA and 5′AGC), the same species (11*S*,3′ orientation) of tomaymycin are attached to DNA. While for the case of the 5′CGA bonding sequence, modeling is predictive of the species found; for the 5′AGC bonding sequence, modeling predicts the 11*S*,5′ species by 14.2 kcal/mol over the 11*S*,3′ species. It is not clear why there is such a large discrepancy; however, one possibility is that it is the noncovalent interactions that determine the orientation and configuration of the covalent adduct.

III. Can Tomaymycin Molecules be Bound Tail-to-Tail on Opposite Strands? In principle, two tomaymycin molecules can be juxtapositioned within the 10-mer duplex either in a head-to-head or tail-to-tail configuration on opposite strands of DNA. Conceivably, in two different bonding sequences a head-to-tail or tail-to-head configuration might also be achieved. In this study and the previous one, head-to-head configurations have been predicted and found in practice. For comparison, the two bonding sequences were specifically arranged so that the tails of the drug molecules were predicted to be pointing towards each other (see Scheme IV). As before, molecular modeling was carried out to determine if steric interference would preclude this orientation, and ^{31}P and

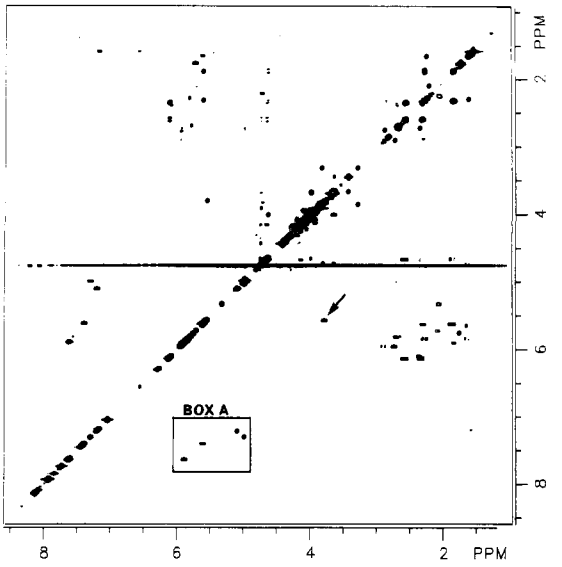

Figure 5. Two-dimensional magnitude COSY contour plot of the bis-tomaymycin 10-mer duplex adduct in 0.5 mL of D_2O buffer containing 10 mM sodium phosphate and 100 mM sodium chloride, pH 6.85 at 23 °C. Box A encloses the four cytosine H5–H6 proton scalar coupling. Arrowhead denotes the scalar coupling indicative of the 11*S* diastereomer between tomaymycin H11 and H11a protons.

Scheme IV

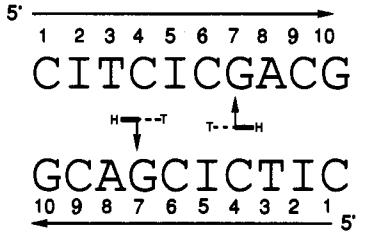

^{1}H NMR was used to determine the complexity and, if possible, the identity of the species bound.

A. Molecular Modeling. The four possible species (11*S*,3′; 11*S*,5′; 11*R*,3′; 11*R*,5′) of tomaymycin on the 10-mer were modeled using AMBER 3A. None of the possible species show unacceptable steric interactions. The results in Table V show that three of the species are within 7.6 kcal/mol, and the 11*S*,3′ and the 11*S*,5′ species are 1.5 kcal/mol Å apart in energy. These small energy differences

Table V. Energies (kcal/mol) of Covalent Complexes between Tomaymycin and d(CITCICGACG)$_2$

direction of aryl ring	config at C-11	drug–drug orientation	total energy	intermolecular			distortion			net bonding energy[e]
				vdw[a]	elstat[b]	total	helix[c]	drug[d]	total	
3′	R	tail–tail	−687.5	−40.8	−23.9	−64.7	+25.5	+7.2	+32.7	−32.0
3′	S	tail–tail	−707.9	−54.0	−30.0	−84.0	+26.1	+6.6	+32.7	−51.3
5′	R	head–head	−700.7	−38.9	−44.7	−83.6	+26.3	+12.1	+38.4	−45.2
5′	S	head–head	−709.4	−57.7	−35.5	−93.2	+29.0	+11.4	+40.4	−52.8

[a] Van der Waals or steric contribution. [b] Electrostatic contribution. [c] The enthalpy of d(CITCICGACG)$_2$ is −695.8 kcal/mol. [d] The enthalpy of the drug molecule in the absence of the DNA is +22.4 kcal/mol. [e] Net bonding is the total intermolecular bonding plus helix and drug distortion.

Table VI. Energies (kcal/mol) of *S*, 3′ Head-to-Head Covalent Complexes between Tomaymycin Crosslinkers and d(CICGATCICG)$_2$

model designation	(-CH_2-) units	total energy	intermolecular			distortion			linker energy[e]	net bonding energy[f]
			vdw[a]	elstat[b]	total	helix[c]	drug[d]	total		
ethyl	2	-690.1	-43.5	-28.8	-72.3	+25.4	+11.2	+36.6	+3.1	-32.6
propyl	3	-690.5	-40.9	-29.1	-70.0	+22.0	+11.4	+33.4	-0.6	-37.2
butyl	4	-689.9	-41.5	-27.7	-69.2	+21.4	+11.7	+33.1	+1.1	-35.0
pentyl	5	-698.7	-47.6	-31.1	-78.7	+20.5	+12.9	+33.4	-3.6	-48.9

[a] Van der Waals or steric contribution. [b] Electrostatic contribution. [c] The enthalpy of d(CICGATCICG)$_2$ is -698.3 kcal/mol. [d] The enthalpy of the drug molecule monomers in the absence of the DNA is +22.4 kcal/mol. [e] The enthalpy contribution of the linker [-$(CH_2)_n$-] atoms only. [f] Net bonding is the total intermolecular bonding plus helix and drug distortion.

suggest that either the 11*S*,3′ or 5′ species may be found experimentally. The main difference between the two species is that the 11*S*,3′ species has less distortion (7.7 kcal/mol Å), but this is offset by the lower intermolecular interaction energy of the 11*S*,5′ species.

B. One-Dimensional ^{31}P and ^{1}H NMR Studies. A comparison of the one-dimensional ^{31}P and ^{1}H NMR spectra of the duplex with the drug-modified duplex adducts shows that the duplex adduct data sets have *at least* twice the complexity of the original duplex set (J.-J. Wang, unpublished results). Although a full analysis of two-dimensional data sets was not attempted, it seems likely that both species have the 11*S* stereochemistry, since two partially overlapped C11 and C11a scalar crosspeaks are present in the magnitude COSY spectrum (see arrow in Figure 6). The loss of self-complementarity of the bis-tomaymycin duplex adduct is further evident in the magnitude COSY, because at least eight scalar cross-peaks for the four cytosine 5H–6H protons are present (box A in Figure 6). Therefore, in contrast to the head-to-head configurations, and using the same bonding sequences and a similar interdrug distance, the predicted tail-to-tail configuration of drug molecules results in loss of duplex self-complementarity. This may be because there are two different species (e.g., 11*S*,3′ and 5′) on this duplex or that the species are the same (e.g., 11*S*,3′), but the juxtaposition of the two drug molecules caused distortion of the helix.

IV. Design of a DNA–DNA Interstrand Guanine–Guanine Cross-Linker Based Upon the Head-to-Head Linking of Two Tomaymycin Molecules. Based upon the studies described in this investigation, the 10-mer duplex containing either a 5′CGA or 5′AGC sequence could in principle serve as a duplex template for the design of a tomaymycin DNA–DNA interstrand cross-linker where the two monoadducts are covalently bound four base-pairs apart on opposite strands in a head-to-head orientation. The stereochemistry at the covalent linkage site is defined as 11*S*, and the drugs are orientated with the aromatic rings pointed to the 3′ sides of the covalently modified guanines (see Figure 7). Because the 10-mer duplex maintains a B-type structure and drug modification of the DNA minimally distorts the helix, the computer-assisted drug design is a relatively straightforward process. As we noted in previous studies,[2,3] substituents at the 8-position on the aromatic ring point along the minor groove of DNA, and in the case of the bis-tomaymycin–duplex adduct, point towards the aromatic ring of the drug on the opposite strand. The molecular modeling was carried out by removal of the proton from each 8-phenol group and linking the two unmasked oxygens with an alkane [$(CH_2)_n$] linker, where n = 2, 3, 4, and 5. Distances between the 8-phenolic group oxygens of the two tomaymycin molecules in the 11*S*,3′CGA and 11*S*,3′AGC adduct models were 6.77 and 7.01 Å, respectively. Using straight-chain diols as models, a two-carbon methylene chain (n = 2) provides approximately 3.6 Å between the oxygen atoms. Similarly, a five-carbon methylene unit (n = 5) yields approximately 7.4 Å between oxygen atoms. Thus, the optimal chain

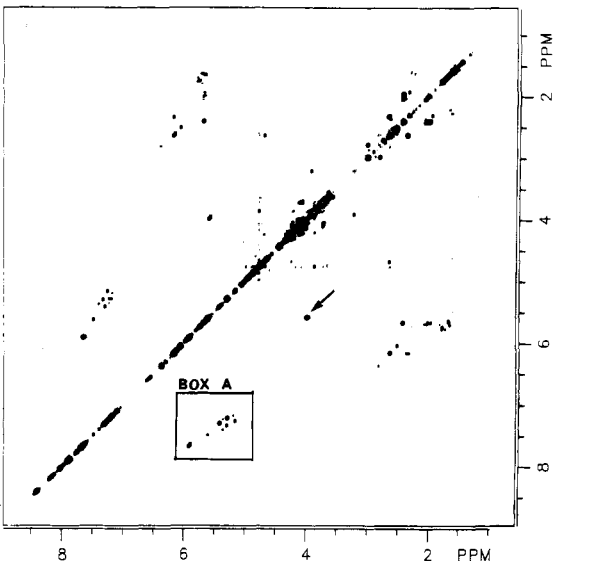

Figure 6. Two-dimensional magnitude COSY contour plot of the bis-tomaymycin 10-mer duplex adduct in 0.5 mL of D_2O buffer containing 10 mM sodium phosphate and 100 mM sodium chloride, pH 6.85 at 23 °C. Arrowhead denotes coupling between the tomaymycin H11 and H11a protons indicative of at least one distinct 11*S* diastereomeric species. Box A encloses the cytosine H5–H6 proton scalar coupling, indicating at least two different drug species.

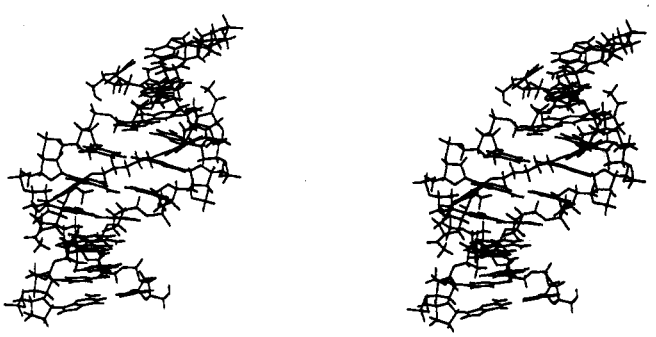

Figure 7. Stereopair of the DNA–DNA 10-mer interstrand cross-linked [(-CH_2-)$_5$] bis-tomaymycin (5′CGA head-to-head) duplex adduct designed by computer-assisted molecular modeling.

length for linking two tomaymycin molecules on these 10-mers would be expected at about n = 4 or 5. Models of each of these cross-linkers were made and subjected to minimization with 55 ps of molecular dynamics and reminimization as before. The results in Table VI show a clear preference for the model in which n = 5. This pentyl model is some 11.5 kcal/mol more stable than the other shorter chain models. At n > 5, the linkers become too "floppy" and the correct orientation becomes more difficult to attain. General trends in the results are that helix distortion decreases as chain length increases, and while total distortion for the propyl, butyl, and pentyl models are nearly identical, it is the increase in intermolecular interactions that finally favors the pentyl model.

We have recently shown that the structurally simplified P[1,4]B cross-linker DSB-120[23] (II) (Figure 8) can form a DNA-DNA interstrand cross-linker between guanines in the 10-mer duplex shown in Scheme II without appreciable distortion of the duplex, as predicted by this combined NMR and molecular modeling study (Wang and Hurley, unpublished results). This compound is considerably more potent that the monoalkylation compound and is not expected to show the cardiotoxicity previously associated with anthramycin and sibiromycin.[13]

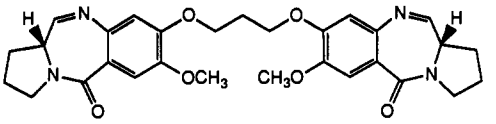

Figure 8. Structure of DSB-120 (II).[23]

Acknowledgment. Supported by grants from the National Cancer Institute (CA-49751), the Welch Foundation, the Burroughs Wellcome Fund, and The Upjohn Company. We are grateful to Steve D. Sorey for technical assistance and David M. Bishop for preparation of the manuscript.

(23) Bose, D. S.; Thompson, A. S.; Ching, J.; Hartley, J. A.; Berardini, M. D.; Jenkins, T. C.; Neidle, S.; Hurley, L. H.; Thurston, D. E. Rational Design of a Highly Efficient Non-Reversible DNA Interstrand Cross-Linking Agent Based on the Pyrrolobenzodiazepine Ring System. *J. Am. Chem. Soc.* **1992**, *114*, 4939-4941.

Synthesis and Antifolate Evaluation of 10-Ethyl-5-methyl-5,10-dideazaaminopterin and an Alternative Synthesis of 10-Ethyl-10-deazaaminopterin (Edatrexate)

J. R. Piper,*,† C. A. Johnson,† G. M. Otter,‡ and F. M. Sirotnak‡

Kettering-Meyer Laboratory, Southern Research Institute, Birmingham, Alabama 35255, and Memorial Sloan-Kettering Cancer Center, New York, New York, 10021. *Received March 26, 1992*

Previous findings suggesting that 5,10-dialkyl-substituted derivatives of 5,10-dideazaaminopterin warranted study as potential antifolates prompted synthesis of 10-ethyl-5-methyl-5,10-dideazaaminopterin (**12a**). The key step in the synthetic route to **12a** was Wittig condensation of the tributylphosphorane derived from 6-(bromomethyl)-2,4-diamino-5-methylpyrido[2,3-*d*]pyrimidine (**7a**) with methyl 4-propionylbenzoate. Reaction conditions for the Wittig condensation were developed using the tributylphosphorane prepared from 6-(bromomethyl)-2,4-pteridinediamine (**7b**) as a model. Each of the respective Wittig products **8a** and **8b** was obtained in 75–80% yield. Hydrogenation of **8a** and **8b** at their 9,10-double bond afforded 4-amino-4-deoxy-10-ethyl-5-methyl-5,10-dideazapteroic acid methyl ester (**9a**) and 4-amino-4-deoxy-10-ethyl-10-deazapteroic acid methyl ester (**9b**). This route to **9b** intersects reported synthetic approaches leading to 10-ethyl-10-deazaaminopterin (10-EDAM, edatrexate), an agent now in advanced clinical trials. Thus the Wittig approach affords an alternative synthetic route to 10-EDAM. Remaining steps were ester hydrolysis of **9a,b** to give carboxylic acids **10a,b** followed by standard peptide coupling with diethyl L-glutamate to produce diethyl esters **11a,b**, which on hydrolysis gave **12a** and 10-EDAM (**12b**), respectively. The relative influx of **12a** was enhanced about 3.2-fold over MTX, but as an inhibitor of dihydrofolate reductase (DHFR) from L1210 cells and in the inhibition of L1210 cell growth in vitro, this compound was approximately 20-fold less effective than MTX (DHFR inhibition, K_i = 4.82 ± 0.60 pM for MTX, 100 pM for **12a**; cell growth, IC_{50} = 3.4 ± 1.0 nM for MTX, 65 ± 18 nM for **12a**).

The classical antifolate methotrexate (MTX), an inhibitor of dihydrofolate reductase (DHFR), remains the only folate analogue in established clinical use for the treatment of cancer. Because of the vital centrality of folate-dependent enzymes in cell proliferation, folate antimetabolites offer high therapeutic promise, especially if greater selectivity of antitumor action can be achieved. Recent investigations have included efforts to identify patterns of structural modifications in those antifolate candidates which have greater antitumor selectivity than MTX.[1,2]

Positions 5 and 10 of classical antifolates are sites where modifications can be made that affect cellular uptake and retention of the candidate drugs without compromising effective binding and inhibition of DHFR.[1] Some analogues modified at these positions are known to accumulate at greater differential levels relative to MTX in tumor than in normal proliferative tissue.[3-6] In a highly responsive tumor, both membrane transport and FPGS work in tandem to provide high levels of the 4-aminofolates.[1,7-10]

These differences between tumor and normal tissues and the enhancement of the accumulation differential through structural modification were exploited in the 10-deazaaminopterin series. This series, particularly the 10-ethyl analogue (10-EDAM), exhibited markedly enhanced

† Southern Research Institute.
‡ Memorial Sloan-Kettering Cancer Center.

(1) Sirotnak, F. M.; DeGraw, J. I. Selective Antitumor Action of Folate Analogs. In *Folate Antagonists as Therapeutic Agents*; Sirotnak, F. M., Burchall, J. J., Ensminger, W. D., Montgomery, J. A., Eds.; Academic Press: Orlando, FL, 1982; Vol. 2, pp 43-95.

(2) Berman, E. M.; Werbel, L. M. The Renewed Potential for Folate Antagonists in Contemporary Cancer Chemotherapy. *J. Med. Chem.* **1991**, *34*, 479-485.

(3) Sirotnak, F. M.; Schmid, F. A.; Otter, G. M.; Piper, J. R.; Montgomery J. A. Structural Design, Biochemical Properties, and Evidence for Improved Therapeutic Activity of 5-Alkyl Derivatives of 5-Deazaaminopterin and 5-Deazamethotrexate Compared to Methotrexate in Murine Tumor Models. *Cancer Res.* **1988**, *48*, 5686-5691.

(4) Sirotnak, F. M.; DeGraw, J. I.; Moccio, D. M.; Samuels, L. L.; Goutas, L. J. New folate analogs of the 10-deaza-aminopterin series. Basis for structural design and biochemical and pharmacologic properties. *Cancer Chemother. Pharmacol.* **1984**, *12*, 18-25.

(5) Sirotnak, F. M.; DeGraw, J. I.; Schmid, F. A.; Goutas, L. J.; Moccio, D. M. New folate analogs of the 10-deaza-aminopterin series. Further evidence for markedly increased antitumor efficacy compared with methotrexate in ascitic and solid murine tumor models. *Cancer Chemother. Pharmacol.* **1984**, *12*, 26-30.

0022-2623/92/1835-3002$03.00/0